Analysis of Adaptive Individual Pitch Control Schemes for Blade Fatigue Load Reduction on a 15 MW Wind Turbine

Lara, Manuel; Mulders, Sebastiaan Paul; van Wingerden, Jan Willem; Vázquez, Francisco; Garrido, Juan

DOI
10.3390/app14010183

Publication date
2024

Document Version
Final published version

Published in
Applied Sciences (Switzerland)

applied sciences

MDPI

Article

Analysis of Adaptive Individual Pitch Control Schemes for Blade Fatigue Load Reduction on a 15 MW Wind Turbine

Manuel Lara [1], Sebastiaan Paul Mulders [2], Jan-Willem van Wingerden [2], Francisco Vázquez [1] and Juan Garrido [1,*]

[1] Department of Electrical Engineering and Automation, University of Cordoba, Campus of Rabanales, 14071 Cordoba, Spain; p12laorm@uco.es (M.L.); fvazquez@uco.es (F.V.)
[2] Delft Center for Systems and Control, Faculty of Mechanical Engineering, Delft University of Technology, Mekelweg 2, 2628 CD Delft, The Netherlands; s.p.mulders@tudelft.nl (S.P.M.); j.w.vanwingerden@tudelft.nl (J.-W.v.W.)
* Correspondence: juan.garrido@uco.es; Tel.: +34-957218729

Abstract: Individual pitch control (IPC) is a method to mitigate periodic blade loads in wind turbines, and it is typically implemented using the multi-blade coordinate (MBC) transform, which converts the blade load measurements from a rotating frame into the non-rotating tilt axis and yaw axis. Previous studies have shown that by including an additional tuning parameter in the MBC, the azimuth offset reduces the coupling between non-rotating axes, allowing for higher performance levels for diagonal controller structures. In these studies, the decentralized control of IPC was composed of two identical integral controllers. This work analyzes and compares the improvement that the azimuth offset can provide in different adaptive gain scheduling IPCs where the diagonal controllers can have integral or proportional action with different gains. They are applied to a 15 MW wind turbine simulated with OpenFAST v3.5 software. The controller parameter tuning is addressed as an optimization that reduces blade fatigue load based on the damage equivalent load (DEL) and is resolved through genetic algorithms. Simulations show that only using different controller gains in IPC does not provide significant improvements; however, including azimuth offset in the optimal IPC schemes with integral controllers allows for the greatest DEL reduction with a lower actuator effort.

Keywords: wind turbine control; individual pitch control; blade load reduction; genetic algorithms; gain-scheduling control

Citation: Lara, M.; Mulders, S.P.; van Wingerden, J.-W.; Vázquez, F.; Garrido, J. Analysis of Adaptive Individual Pitch Control Schemes for Blade Fatigue Load Reduction on a 15 MW Wind Turbine. *Appl. Sci.* **2024**, *14*, 183. https://doi.org/10.3390/app14010183

Academic Editors: Galih Bangga and Martin Otto Laver Hansen

Received: 11 December 2023
Revised: 20 December 2023
Accepted: 24 December 2023
Published: 25 December 2023

1. Introduction

Currently, global warming and climate change are major concerns that are driving efforts to reduce greenhouse gas emissions. Since energy generation accounts for approximately 30% of these emissions, wind energy has been a key renewable energy source from the outset [1]. In 2021, wind power capacity worldwide reached 837 GW, with the USA, China, India, Germany, and Spain representing 72% of it. However, the International Energy Agency forecasts that by 2030, wind power capacity needs to reach 3200 GW to limit the temperature increase to 1.5 °C [2]. In 2021, the EU introduced a plan to lower net greenhouse gas emissions by 2030 by at least 55%. The arrangement incorporates more investment in clean energy, and by 2030, onshore and offshore wind power is expected to produce 25% of the EU's renewable energy [3]. The main new developments in wind energy technology have involved increasing the size of wind turbines, which has increased energy generation and energy efficiency but has created challenges for maintenance and operation. To make this expansion economically affordable and competitive, the operation of wind turbines must be more efficient.

Currently, new wind turbines are becoming larger and more flexible. Consequently, reducing their fatigue loadings to extend their lifetime has become particularly important. If the structural loads of wind turbines are not relieved, their overall performance may

deteriorate or premature failure may occur. Therefore, it is important to understand how structural stresses affect wind turbine output and equipment life. Various deflection modes of towers, rotors, blades, and vibrations of turbine drive trains are the most typical phenomena and can result in different types of structural stresses [1]. From a control viewpoint, the service life of wind turbines can be extended by reducing various structural loads.

Currently, wind turbines with three rotor blades and variable speed and variable blade pitch (VS-VP) on a horizontal axis are the most common. This study focuses on the full-load region, where it is essential to minimize the negative effects of high wind speeds to prevent system damage. Traditionally, wind turbines operating in this region use collective pitch control (CPC) for speed control. However, most modern wind turbines now have independent pitch control (IPC) mechanisms for each blade. IPC can provide advantages because it can help decrease the stress on the rotor blades, hubs, and tower structures without having significant effects on the generated power.

There are two types of blade fatigue loads: in-plane and out-of-plane. These loads primarily arise at integer multiples of the turbine's rotational speed (n-P) [4]. As illustrated in Figure 1a [5], these components have different directions: The out-of-plane (OoP) component is aligned in the direction perpendicular to the plane of rotation, whereas the in-plane component is aligned in the direction tangential to it. Sensors installed on each blade can measure the bending moment. Nevertheless, as shown in Figure 1b [6], where the OoP moment at the root of the i-th blade is referred to as M_{yi}, the respective rotating coordinate frame of each blade affects these measurements.

Most research on IPC uses the azimuth-dependent multi-blade coordinate (MBC) transform, which converts the blade rotating moments into two components in a non-rotating reference system [7]. In this frame, a multivariable controller in IPC is implemented to decrease these two moment components. Although decoupling between these components is expected, in practical scenarios, there is still coupling in the resulting transformed system [4,8]. Some authors have shown that the decoupling of the fixed-frame multivariable system can be improved by using an azimuth offset as an extra parameter in the reverse MBC transformation. In [7], by introducing an azimuth offset in the MBC transformation, the coupling for the 1P harmonic was minimized, which led to advantages in pitch performance and blade fatigue load reduction. In [9], the authors extended previous work and demonstrated the impact and importance of incorporating an azimuth offset to reduce higher periodic harmonics.

Some studies have combined MBC conversion and control techniques, such as linear quadratic Gaussian control [4], model predictive control [10], and the H_∞ technique [8]. Computational intelligence methods, such as artificial neural networks, fuzzy logic, genetic algorithms, particle swarm optimization, decision-making techniques, and statistical methods, are gaining popularity as alternatives to wind turbine control problems. These methods can help improve the performance, reliability, and efficiency of wind turbines by optimizing their control systems, reducing maintenance costs, and increasing their lifespan [11,12]. In [13], Bayesian optimization is used to tune the gains of decentralized integral control and azimuth offset in an IPC scheme to reduce blade fatigue at 1P and 2P loads. The authors demonstrated that their scheme with the azimuth offset outperformed the same scheme without the azimuth offset and the same integral gains. In our previous work [14], we optimized both schemes according to the same cost function and demonstrated that including the azimuth offset provided a reduction of approximately 10% in blade fatigue load and pitch signal effort compared with the optimized IPC scheme without offset. All of these previous studies on IPC force the elements of decentralized control to be pure integral controllers with the same gain. This may be a limitation in achieving better IPC performance that has not yet been addressed.

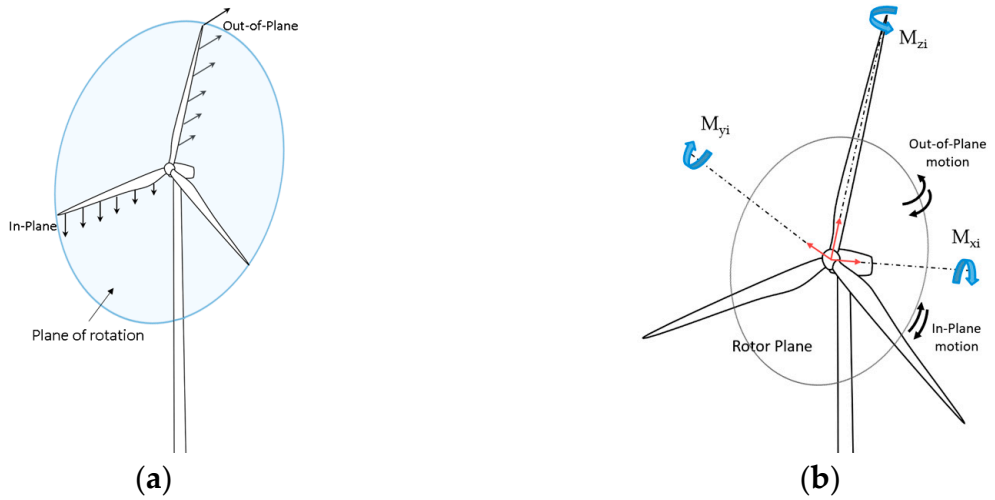

Figure 1. (**a**) Aerodynamic load components on the blades of a wind turbine: perpendicular to the plane of rotation (or out-of-plane) and parallel to it (or in-plane); (**b**) rotating reference frame of the i-th blade. For the i-th blade, the in-plane moment is symbolized by M_{xi} and its out-of-plane bending moment by M_{yi} [14].

This work analyzes different simple IPC schemes where the decentralized controllers can have integral or proportional action with different gains. Furthermore, they may include the azimuth offset to improve the IPC response. To perform a fair comparison, all of the parameters of the different schemes are optimized with Gas to minimize fatigue on the OoP blade loads according to the DEL [15]. The proposed schemes are applied to the International Energy Agency (IEA) 15 MW reference wind turbine (RWT), which is simulated with OpenFAST v3.5 and MATLAB/Simulink R2022b software. The IPCs are designed to adaptively adjust their gain as a function of wind speed in the nominal region due to the system's nonlinearity. The results of all of the schemes are compared with those of a classic baseline CPC PI-controlled turbine without IPC. It is shown that the IPC schemes with integral controllers plus the azimuth offset outperform the other schemes, achieving the greatest reduction in the DEL value of the OoP blade moments using the lowest pitch signal activity. The IPC schemes with proportional controllers exhibit similar performance to the IPC schemes with integral controllers without the azimuth offset. Using different gains in the IPC controllers does not provide advantages compared with the respective IPC schemes with identical decentralized controllers.

The main novelties of this work compared to the available literature are as follows:

- In closely related previous research [14], IPC schemes with two identical pure integral controllers with and without the azimuth offset were compared. In this work, a study in more detail is performed for simple IPC schemes optimized to minimize the fatigue blade load. Specifically, we check the influence of using integral or proportional controllers, tuning them with different gains and including or not including the azimuth offset in the reverse MBC transform. The improvements that can be achieved considering these features are analyzed qualitatively and quantitatively.
- The IPC schemes are implemented as adaptive blocks where the controller gains are scheduled according to the mean value of the measured filtered blade moments instead of the wind speed in the above-rated region.
- Most of the research papers published so far on OpenFAST have concentrated on the 5 MW NREL turbine. However, this study is conducted on a 15 MW turbine, a type of turbine on which not much research has been conducted so far.

The remainder of this article is organized as follows. Section 2 describes the proposed methodology, control schemes, and optimization procedure. Section 3 presents a comparative analysis of the results obtained by the proposed IPC schemes and discusses the

improvements achieved by the optimized IPC schemes when the azimuth offset is included. Finally, we summarize our conclusions in Section 4. Before the references, there is a section listing the nomenclature in this work.

2. MBC Transform

This section provides an overview of the IPC and multi-blade coordination (MBC) transformations in three-blade wind turbines for 1P harmonic blade load mitigation. The azimuth-dependent MBC transform is a mathematical technique for integrating and expressing the dynamics of blades in a fixed (non-rotating) frame. With the MBC transform, the rotating blade moments can be converted into two components in a non-rotating reference frame: the tilt M_t and the yaw M_y moments [7]. In the case of the MBC transform for harmonic 1P, the rotating out-of-plane (OoP) bending moments of the three blades are arranged in the vector $\mathbf{M}(t) = [M_1(t)\ M_2(t)\ M_3(t)]^T$. This vector is then provided to the forward MBC transform matrix $\mathbf{T}(\psi)$ to calculate the azimuth-independent moments in the fixed frame, i.e., $M_t(t)$ and $M_y(t)$. This is illustrated below:

$$\begin{bmatrix} M_t(t) \\ M_y(t) \end{bmatrix} = \boldsymbol{T}(\boldsymbol{\psi})\boldsymbol{M}(t). \tag{1}$$

The three-element vector $\boldsymbol{\Psi}$ is an array with the azimuthal angle of each blade. The vertical upright position of the blade is represented by a zero value for its angle. The forward transformation matrix is given in:

$$\boldsymbol{T}(\boldsymbol{\psi}) = \frac{2}{3}\begin{bmatrix} \cos(\psi_1) & \cos(\psi_2) & \cos(\psi_3) \\ \sin(\psi_1) & \sin(\psi_2) & \sin(\psi_3) \end{bmatrix}. \tag{2}$$

Then, the tilt and yaw pitch angles, $\beta_t(t)$ and $\beta_y(t)$, respectively, are computed typically by a decentralized control in the IPC block in order to reduce the two components M_t and M_y. Subsequently, these two non-rotating pitch signals are converted into the rotational reference system to calculate the IPC components in the rotating frame:

$$\begin{bmatrix} \beta_{IPC1}(t) \\ \beta_{IPC2}(t) \\ \beta_{IPC3}(t) \end{bmatrix} = \boldsymbol{T}^{-1}(\boldsymbol{\psi} + \psi_o)\begin{bmatrix} \beta_t(t) \\ \beta_y(t) \end{bmatrix}. \tag{3}$$

This transformation is calculated by means of the reverse MBC transform, $\mathbf{T}^{-1}$, which is given in Equation (4). The parameter ψ_o is the azimuth offset, which can reduce the coupling effects that remain between the two components in the fixed reference system. Each IPC component is added to the CPC signal β_{CPC} to compute the pitch command value for each blade β_i.

$$\boldsymbol{T}^{-1} = \begin{bmatrix} \cos(\psi_1 + \psi_o) & \sin(\psi_1 + \psi_o) \\ \cos(\psi_2 + \psi_o) & \sin(\psi_2 + \psi_o) \\ \cos(\psi_3 + \psi_o) & \sin(\psi_3 + \psi_o) \end{bmatrix} \tag{4}$$

3. Proposed Methodology

This section explains the proposed methodology: a wind turbine model for testing the method and simulation framework, control system schemes, and an optimization process with GAs.

3.1. Wind Turbine Model and Simulation Framework

The design method proposed in this study is tested on the IEA 15-MW reference wind turbine [16]. This turbine model is co-simulated using MATLAB/Simulink vR2022b and OpenFAST v3.5 software [17]. OpenFAST is an open-source tool created by the National Renewable Energy Laboratory (NREL) for aero-servo-hydro-elastic simulation. The turbine is configured as an offshore monopile wind turbine, and its main specifications are shown

in Table 1. The developed control system is simulated with Simulink, while the wind turbine (rotor, blades, tower, etc.) and wind conditions are simulated with OpenFAST. In this study, still water is assumed, so no wave profile is simulated. This turbine has been garnering more interest in the literature lately [18,19], but compared to the NREL 5 MW wind turbine, there are still few studies on this 15 MW wind turbine [20].

Table 1. IEA 15 MW RTW properties.

Property	Value
Power rating	15 MW
Rotor orientation, configuration	Upwind, 3 blades
Cut-in, rated rotor speed	5 rpm, 7.56 rpm
Cut-in, rated, cut-out wind speed	3 m/s, 10.59 m/s, 25 m/s
Drivetrain	Low speed, direct drive
Rated generator torque	19,786,767.5 Nm
Electrical generator efficiency	95.756%
Rotor, hub diameter, hub height	240 m, 7.94 m, 150 m
Rotor nacelle assembly mass	1,070,000 kg
Tower mass	860,000 kg
Blade pitch angle limits	0–90 deg
Pitch slew-rate limits	2 deg/s
Generator torque slew-rate limits	4,500,000 Nm/s

This study only considers wind turbines operating in the full-load region, where the rotor blades are subjected to the highest damage due to the periodic blade loads that increase with the average wind speed [21]. In this region, the torque controller reaches saturation at the rated torque while a blade pitch proportional–integral (PI) controller acts on the pitch to maintain the rotor speed around its rated value. Because the OpenFAST wind turbine model does not consider the dynamics of the pitch actuators, they are modeled using a second-order unity gain transfer function with a damping factor of 0.707 and a natural frequency of 3.14 rad/s. The IPC is tuned by optimization to minimize the mean DEL value of the OoP blade moments. Simulations for this optimization are performed with stochastic turbulent wind signals generated using TurbSim v2 [22] within the nominal region. Specifically, five operation points are considered according to the following mean wind speeds: 14, 16, 18, 20, and 22 m/s. The wind profiles are designed according to the IEC standard [23] using a Kaimal turbulence spectrum with a hub turbulence intensity of 10% and a vertical shear with a power-law exponent of 0.2. The sample rate is 200 Hz.

3.2. Control System Scheme

The control system proposed in this study is shown in Figure 2. It has two control blocks: a CPC and an IPC. The control signals of these blocks are combined to provide the total pitch command signal β_i for each pitch actuator. As in the full load region, the wind turbine is designed to generate power at the rated power output and the generator torque T_g is set to its nominal value $T_{g,rated}$. Therefore, the generated power (P_g) depends only on the generator speed ω_g according to Equation (5) [24]. If the wind turbine rotation speed is regulated to its rated value $\omega_{g,rated}$, then the power generated can be maintained at the rated value. The CPC generates the same pitch signal β_{CPC} for all blades to maintain this speed at its rated value and rejects changes in wind speed ν.

$$P_{g,rated} = T_{g,rated} \cdot \omega_{g,rated} \quad (5)$$

This study does not consider the CPC tuning procedure. We use a pre-designed CPC PI controller that is reimplemented in Simulink based on the reference open-source controller (ROSCO) implementation. We use the tuning parameters presented in [25], which are adjusted by gain scheduling based on the CPC pitch signal.

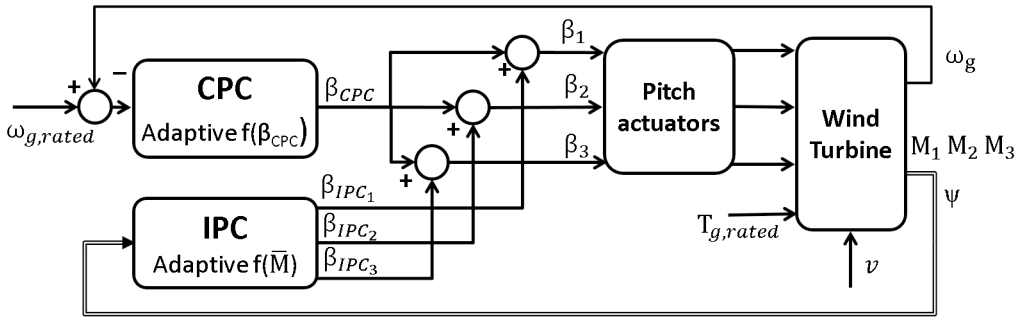

Figure 2. IPC + CPC control scheme for the above-rated region. The CPC supplies a common pitch command angle for the blades to control the rotational speed of the generator at its rated value. The IPC computes an individual action for each blade to decrease the blade moments. Both control actions are combined to provide the total command signals for each pitch actuator of the wind turbine [14].

This work focuses on the design of the IPC block, whose main goal is to reduce blade loads. The proposed IPCs are combined with the pre-designed CPC to run the simulations. The considered IPC scheme is shown in Figure 3. It consists of the MBC transformation for 1P harmonic reduction; a multi-loop control with two controllers, $C_t(s)$ and $C_y(s)$; and the reverse MBC transformation, which can incorporate the azimuth offset ψ_o. From the OoP blade moments (M_1, M_2, and M_3) measured in the rotating frame, the tilt and yaw moments M_t and M_y in the non-rotating frame are computed using the MBC transform. A decentralized control scheme with two controllers provides the tilt and yaw pitch signals (β_t and β_y) to reduce the tilt and yaw moments, respectively. The calculated non-rotating tilt and yaw pitch signals are then transformed into the three different blade pitch angles in the rotating frame using the reverse MBC transform. The decoupling between the pitch and yaw axes can be improved by using the azimuth offset, which can help achieve a greater reduction in the periodic blade loads compared with the IPC schemes without offset ($\psi_o = 0°$). Finally, the IPC signal β_{IPCi} and the CPC value β_{CPC} are added to obtain the total command pitch angle for each blade.

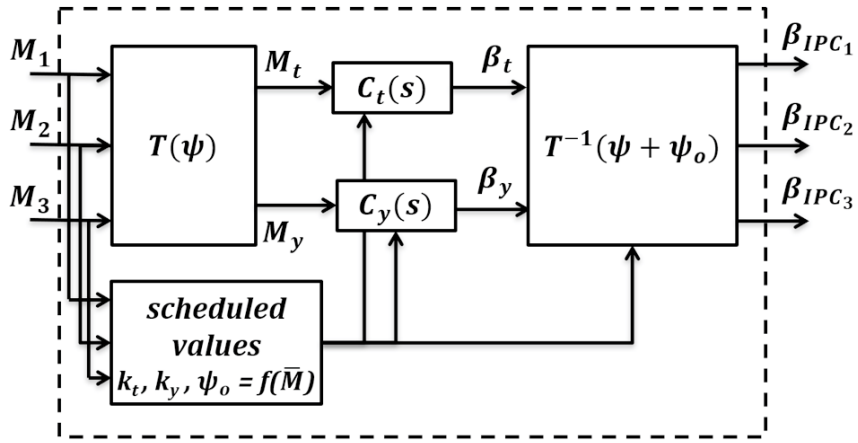

Figure 3. General scheme of the IPC with the azimuth offset in the reverse MBC transform and a decentralized control composed of the controllers $C_t(s)$ and $C_y(s)$. The forward MBC transformation $\mathbf{T}(\psi)$ transforms the 1P harmonics of the OoP blade load moments to a fixed reference system. Then, a decentralized control loop reduces the computed tilt- and yaw-axis moments. By using the reverse MBC transform, these control signals are converted to the rotating frame to obtain the final IPC signals β_{IPCi}. The gains of the decentralized controllers and the azimuth offset are adapted by scheduled values according to the mean value of the filtered moments of the three blades.

In this study, we design and compare six different cases of IPC according to the complexity (the number of degrees of freedom to be tuned) and the type of controller in

the IPC scheme (proportional or integral control). When $C_t(s)$ and $C_y(s)$ are proportional (P) controllers, they are equal to unity and k_t and k_y are proportional gains; when they are integral (I) controllers, $C_t(s) = C_y(s) = 1/s$ and k_t and k_y are integral gains. In addition, IPC schemes can include the azimuth offset ψ_o and can force the gains to have the same value. By combining these three factors (P or I controllers, gains with identical or different values, and including the azimuth offset or not), six cases are proposed for evaluation; the two cases with identical gains and P controllers are not considered. The six proposed cases are the following:

- Control 1 (IPC_P2): The IPC comprises two different P controllers, and no azimuth offset is tuned. Therefore, $C_t(s) = C_y(s) = 1$, $k_t \neq k_y$, and $\psi_o = 0°$. There are only two parameters to be tuned: the controller gains.
- Control 2 (IPC_P2ψ): The IPC comprises two different P controllers and includes the azimuth offset. Therefore, $C_t(s) = C_y(s) = 1$ and $k_t \neq k_y$. There are three parameters to be tuned: the controller gains k_t and k_y and the azimuth offset ψ_o.
- Control 3 (IPC_I1): The IPC is composed of two identical I controllers because they are forced to have the same gain; no azimuth offset is tuned. Therefore, $C_t(s) = C_y(s) = 1/s$, $k_t = k_y$, and $\psi_o = 0°$. There is only one parameter to be tuned: the common controller gain.
- Control 4 (IPC_I1ψ): The IPC is composed of two identical I controllers and includes the azimuth offset. Therefore, $C_t(s) = C_y(s) = 1/s$ and $k_t = k_y$. There are two parameters to be tuned: the common controller gain and the azimuth offset ψ_o.
- Control 5 (IPC_I2): The IPC comprises two different I controllers, and no azimuth offset is tuned. Therefore, $C_t(s) = C_y(s) = 1/s$, $k_t \neq k_y$, and $\psi_o = 0°$. There are two tuning parameters: the controller gains.
- Control 6 (IPC_I2ψ): The IPC comprises two different I controllers and includes the azimuth offset. Therefore, $C_t(s) = C_y(s) = 1/s$ and $k_t \neq k_y$. There are three parameters to be tuned: the controller gains and the azimuth offset ψ_o.

Variations in wind speed modify the wind turbine operating point and, consequently, the control performance is affected. In this work, an adaptive control based on gain-scheduled IPC is proposed for the control system to perform properly under different wind conditions. To create a gain adaptive control system for the IPC that can adjust to changes in wind speed, the controller is tuned for the five operating points based on the previously determined wind conditions. Nevertheless, the wind speed is not used as the scheduling variable; instead, as a novelty of this work, we propose using the mean value $\overline{M}$ of the filtered moments of the blades as the scheduling variable. In the above-rated region, this mean moment practically depends only on the mean wind speed, and the higher the wind speed, the lower the mean moment of the blades. Table 2 shows this relationship for the five operation points in the IEA 15 MW wind turbine. However, it is important to note that the periodic components of these moments, the amplitude of their fluctuations, and their standard deviation increase with wind speed and turbulence; that is why the DEL value of the OoP blade moments also increases, and that is what IPC can help to reduce. Other studies used the mean wind speed as a scheduling variable [26]; however, that requires additional sensors or estimators, whereas the proposed mean moment $\overline{M}$ can be easily calculated from the measurements of the blade moments used for the IPC.

Table 2. Relationship between mean wind speed and mean OoP blade moment for the IEA 15 MW RTW operating in the nominal region.

Mean Wind Speed (m/s)	Mean OoP Blade Moment (MNm)
14	34.94
16	28.68
18	24.03
20	20.33
22	17.23

3.3. IPC Tuning by Optimization

The tuning of the IPC scheme in Figure 3 is performed by an optimization process that aims to reduce blade fatigue loading by considering the OoP blade moments, i.e., the moments on the y-axis of Figure 1b. Damage equivalent load (DEL) is commonly used in wind turbine fatigue testing. It is commonly computed from time domain data to which cycle counting techniques are applied. In the proposed optimization, we calculate the DEL for each OoP blade moment and calculate the mean value; this mean DEL value ($\overline{\mathrm{DEL}}$(M)) is the fitness or cost function J, i.e., the function to be minimized. This cost function is not analytically assessable because the DEL value is calculated from the time series of the simulation data after the simulation is completed. The MLife script set [27] is used for the post-processing of simulation data to calculate the corresponding DEL. The proposed optimization problem is expressed as follows:

$$\begin{gathered} min\ \overline{DEL}(M) = \frac{1}{3}\sum_{i=1}^{3} DEL(M_i(\boldsymbol{\rho})) \\ subject\ to \\ \text{solution of the model} \\ \boldsymbol{\rho} \in S \end{gathered} \tag{6}$$

The tuning parameters of the IPC define the vector $\boldsymbol{\rho}$ of the decision variables. Depending on the proposed IPC scheme, the dimensionality of the parameter vector varies from one to three. Therefore, the solution space S is restricted to $S \in \mathbb{R}^1$ for the case with only one gain to be tuned ($k_t = k_y$ and $\psi_o = 0$), $S \in \mathbb{R}^2$ for the cases with two different gains ($k_t \neq k_y$ and $\psi_o = 0$) or one gain and one offset ($k_t = k_y$ and $\psi_o \neq 0$), and $S \in \mathbb{R}^3$ for the case with two different gains and one offset ($k_t \neq k_y$ and $\psi_o \neq 0$). The mean DEL value, which is influenced by the parameter vector ρ, should be reduced while taking into account the dynamic behavior of the wind turbine model and the control system and subjected to the solution space S.

Since the cost function J and the wind turbine dynamic model in OpenFAST are very complex and cannot be evaluated analytically, the proposed optimization is performed using the simulation-based approach depicted in Figure 4. First, the initial values of the decision variables are arranged in the vector ρ_0. The optimization procedure then initiates an iterative loop. In this loop, the optimizer runs various simulations in MATLAB using OpenFAST/Simulink, calculates the objective function J, and searches for the optimal solution ρ*. This process results in a nonlinear problem that needs a large amount of calculation and time. In this work, genetic algorithms (GA) are used to perform optimization and improve computational efficiency.

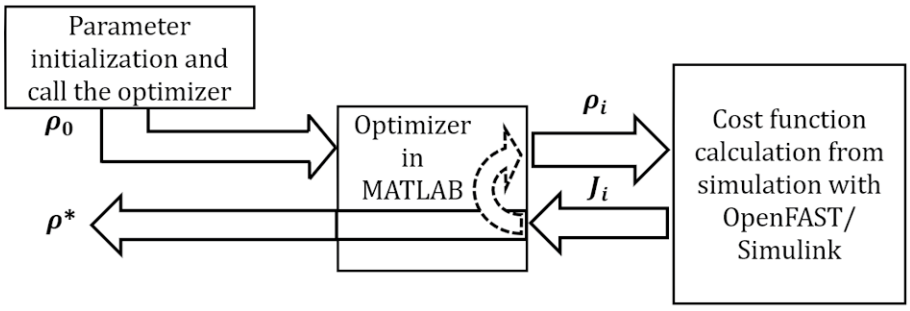

Figure 4. Simulation-based optimization process: First, parameters are initialized, and then, the optimizer in MATLAB performs iterative co-simulations in OpenFAST/Simulink until the optimal parameters that minimize the cost function (the mean DEL of the blade moments) are found.

The different IPC schemes are optimized by simulating the IEA 15 MW WT model at the five previously defined operating points. Each simulation lasts for 800 s, with the first 200 s removed to eliminate transient effects. The optimal parameters for each

operation point are used to implement the adaptive IPC by a gain-scheduled strategy, which computes the required control parameters by linear interpolation of the optimal parameters as a function of the mean value $\overline{M}$ of the filtered blade moments.

3.4. Optimization Algorithm

The optimization process proposed in this study is a complex nonlinear problem that demands significant computation work. To enhance computational efficiency, the optimizer in Figure 4 employs a genetic algorithm that is implemented using the MATLAB Global Optimization Toolbox. Among stochastic global search optimization techniques, genetic algorithms are bio-inspired algorithms that emulate the processes of replication, crossover, and mutation that occur in natural selection and inheritance [28]. These optimization methods are designed to solve complex optimization problems that involve evaluating the cost function using simulation data and simulation-based approaches. GA generates new populations from a previous solution using selection, crossover, mutation, and migration criteria [29]. GA is based on improving the initial population so that, in each iteration, the algorithm achieves the best result. A population is made up of individuals called chromosomes, and each chromosome is encoded as an array of parameters, representing a possible solution. For problems with N dimensions, each chromosome is typically encoded as an array of N elements, where the i-th one is the specific value of the i-th parameter. In the proposed optimization, the chromosome consists of the elements of vector ρ, which can be composed of one, two, or three elements (k_t, k_y, and/or ψ_o), depending on the IPC case. Figure 5 shows the GA steps for the proposed optimization. These steps are:

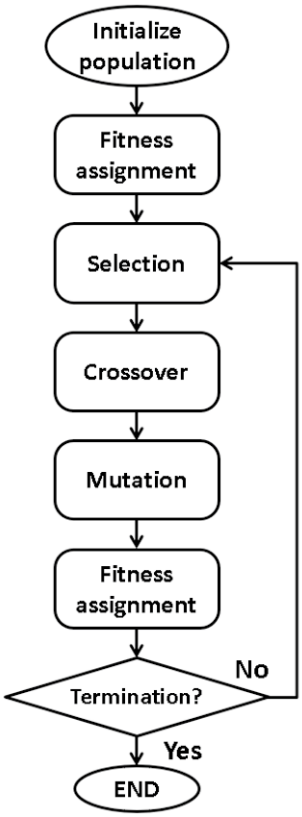

Figure 5. GA steps: population initialization; computation of individual fitness based on the cost function; selection, which is the process for choosing the best individuals and discarding others; generation of a new population by mating the chosen candidates (crossover) and supplying randomness to the new offspring (mutation); and assessment of the new individuals. Iterations continue until the stopping condition is fulfilled [14].

1. Initial population: Before optimization, the tuning parameter search range is set manually using a bisection-type procedure, where the range is reduced by eliminating parameter values that cause instability during simulation. The search interval for the gains is [0–0.3] deg/(MN·m·s) for integral controllers or [0–2] deg/(MN·m) for proportional controllers, and the range for the azimuth offset is [0–90] deg. An initial population of 100 individuals is created with parameter values evenly spaced within the defined range; the population size is 200 for the IPC cases with three parameters to be tuned.
2. Fitness assignment: After initialization, every individual in the population or chromosome is assigned a fitness value. When using a simulation-based approach, the fitness value of each member is calculated by running a simulation. The fitness function is equivalent to the cost function J being optimized.
3. Selection: Its purpose is to select the most suitable individuals and pass on their genes to the following generation. This study uses the roulette selection method, which assigns a higher probability of fitness to chromosomes with lower fitness values, making them more likely to be chosen. The fitness probability of the i-th individual is represented by $P_i = J_i/\sum_{j=1}^{N} J_j$ and its corresponding cumulative fitness probability $q_i = \sum_{j=1}^{i} P_j$. Subsequently, a selection is made by considering the previous probability value's position in the roulette, represented on a cumulative probability of suitability scale. For this purpose, a pseudo-random number r uniformly distributed over the interval [0, 1] is generated. If $q_{k-1} \leq r \leq q_k$, then the k-th candidate is chosen as a parent. In order to reach the required number of parents, the number r is generated multiple times. The best chromosomes are always retained in the population (elite selection). The number of elite individuals in the population is set to 0.05 times the population size.
4. Crossover: This operator creates part of a new population by recombining the selected individuals after sorting and rejecting the chromosomes. For each parent couple (mum and dad), defined in Equation (7), a random gene-crossing point, defined by the random variable α, is chosen before mating. The mom and dad are denoted by subscripts m and d, respectively. The selected parameters $p_{m,\alpha}$ and $p_{d,\alpha}$ are grouped according to Equation (8) to generate new values, p_{new1} and p_{new2}, which appear in the descendants. The parameter γ is a random number within the range of [0, 1]. Then, as shown in Equation (9), the mating process is completed by exchanging other genes (parameters) and obtaining offspring. The crossover fraction is set to 0.75, which represents the fraction of the population created by this operator.

$$\begin{aligned} \mathbf{mom} &= \begin{bmatrix} p_{m,1} & p_{m,2} & \cdots & p_{m,\alpha} & \cdots & p_{m,N} \end{bmatrix} \\ \mathbf{dad} &= \begin{bmatrix} p_{d,1} & p_{d,2} & \cdots & p_{d,\alpha} & \cdots & p_{d,N} \end{bmatrix} \end{aligned} \tag{7}$$

$$\begin{aligned} p_{new1,\alpha} &= p_{m,\alpha} - \gamma(p_{m,\alpha} - p_{d,\alpha}) \\ p_{new2,\alpha} &= p_{d,\alpha} - \gamma(p_{m,\alpha} - p_{d,\alpha}) \end{aligned} \tag{8}$$

$$\begin{aligned} \mathbf{offspring}_1 &= \begin{bmatrix} p_{m,1} & p_{m,2} & \cdots & p_{new1,\alpha} & \cdots & p_{d,N} \end{bmatrix} \\ \mathbf{offspring}_2 &= \begin{bmatrix} p_{d,1} & p_{d,2} & \cdots & p_{new2,\alpha} & \cdots & p_{m,N} \end{bmatrix} \end{aligned} \tag{9}$$

5. Mutation: Transfer a small amount of randomness to new individuals to maintain diversity within the population and avoid locally optimal tracking such as crossover. The mutation probability is set to 0.2.
6. New individual generation: The process of genetic recombination involves the creation of new populations by recombining the resultant offspring with other mutated offspring. This process is repeated until the termination condition is met. This process stops when the fitness of a particular solution achieves the desired level of fitness, the number of generations reaches a maximum limit, or the population becomes stable. In this work, after reaching 20 generations without changes in the best fitness, the process stops because it has been observed that this number is sufficient for convergence in the proposed optimization.

4. Results and Discussion

This section shows the results of the proposed optimization and the comparative analysis and evaluation of the different IPC schemes. After discussing the optimization results, the proposed controllers are tested in different simulations and the temporal responses of the main variables in the rotating frame are then analyzed. The responses of the variables associated with the fixed frame are also compared. Finally, an analysis of the OoP blade moments and pitch signals in the frequency domain is shown.

4.1. Optimization Results

Table 3 shows the tuning parameters obtained after optimization of the six proposed IPC schemes for the five operation points in the above-rated region, which are discussed and collected in Table 2. The mean DEL values of the OoP blade moments are also shown. The DEL values obtained for the CPC without any IPC are listed, as well as those for the baseline case. A graphical representation of these data is shown in Figure 6, which shows the IPC gains, azimuth offset, and mean DEL values with respect to the mean wind speed. From these data, the following points can be stated:

- The IPC schemes with integral controllers plus the azimuth offset (IPC_I1ψ and IPC_I2ψ) achieved the largest reductions in the mean DEL value at all operating points evaluated. The average reduction was 41% with respect to the CPC case. The third best scheme was the IPC with P controllers and the azimuth offset (IPC_P2ψ), which showed an average reduction of 35% in the mean DEL value.
- The IPC schemes with integral action and without the azimuth offset showed the lowest gains and the lowest DEL reductions—only 30% on average. Including the azimuth offset in these schemes allowed the optimal designs to achieve higher gains.
- The two IPC schemes with integral controllers and the azimuth offset (IPC_I1ψ and IPC_I2ψ) had practically the same azimuth offset values ψ_o at each operation point. In the IPC scheme with proportional controllers plus the azimuth offset (IPC_P2ψ), the values of ψ_o were practically zero at all operation points except at 20 m/s. Even so, there did not seem to be much effect on the results when it was set to zero. This is because the integral action adds phase delay, whereas the proportional action does not.
- On the contrary, if we compare the IPC cases with integral controllers, the inclusion of the azimuth offset allowed an increase in the average DEL reduction of the OoP blade moments of about 10% more compared to the same scheme without the offset. Schemes IPC_I1 and IPC_I2 had an average DEL reduction of approximately 30%, but their respective cases with the azimuth offset (IPC_I1ψ and IPC_I2ψ) had an average reduction of 41%.
- Of the two best IPC schemes (IPC_I1ψ and IPC_I2ψ), the IPC_I1ψ case could be considered the most advisable, because, having achieved similar results, it had only two parameters to adjust. It does not seem worthwhile to let the integral gains be different (case IPCI2_ψ) since it does not provide significant improvements and requires the three parameters to be tuned. Furthermore, it was observed that the gains of both k_t and k_y were practically the same at several operating points.

Table 3. Optimization results for different IPC schemes at the five operation points. For each IPC scheme and each operation point, the following elements are listed: the mean DEL value of the OoP blade moment, the decentralized controller gains k_t and k_y, and the azimuth offset ψ_o. The mean DEL values for CPC without IPC are also shown.

Control Scheme		Wind Speed (m/s)				
		14	**16**	**18**	**20**	**22**
CPC	$\overline{\mathbf{DEL}}$**(M) (MNm)**	24.07	23.08	25.06	30.8	25.39
CPC + IPC_P2	$\overline{\mathbf{DEL}}$**(M) (MNm)**	16.91	14.97	17.26	22.06	13.84
	$\mathbf{k_t}$ **(deg/(MNm))**	$18.94 \cdot 10^{-2}$	$19.22 \cdot 10^{-2}$	$23.72 \cdot 10^{-2}$	$8.4 \cdot 10^{-2}$	$14.21 \cdot 10^{-2}$
	$\mathbf{k_y}$ **(deg/(MNm))**	$31.61 \cdot 10^{-2}$	$17.12 \cdot 10^{-2}$	$11.53 \cdot 10^{-2}$	$4.2 \cdot 10^{-2}$	$25.36 \cdot 10^{-2}$
	$\boldsymbol{\psi_o}$ **(deg)**	0	0	0	0	0
CPC + IPC_P2ψ	$\overline{\mathbf{DEL}}$**(M) (MNm)**	16.9	14.9	17.23	20.87	13.84
	$\mathbf{k_t}$ **(deg/(MNm))**	$17.35 \cdot 10^{-2}$	$17.13 \cdot 10^{-2}$	$23.65 \cdot 10^{-2}$	$9.6 \cdot 10^{-2}$	$14.66 \cdot 10^{-2}$
	$\mathbf{k_y}$ **(deg/(MNm))**	$29.07 \cdot 10^{-2}$	$21.97 \cdot 10^{-2}$	$11.54 \cdot 10^{-2}$	$11.2 \cdot 10^{-2}$	$25.69 \cdot 10^{-2}$
	$\boldsymbol{\psi_o}$ **(deg)**	0.55	0.17	5.66	19.36	0.01
CPC + IPC_I1	$\overline{\mathbf{DEL}}$**(M) (MNm)**	17.00	16.27	18.74	22.32	16.73
	$\mathbf{k_t}$ **(deg/(MNms))**	$2.98 \cdot 10^{-2}$	$2.5 \cdot 10^{-2}$	$0.93 \cdot 10^{-2}$	$0.77 \cdot 10^{-2}$	$0.49 \cdot 10^{-2}$
	$\mathbf{k_y}$ **(deg/(MNms))**	$2.98 \cdot 10^{-2}$	$2.5 \cdot 10^{-2}$	$0.93 \cdot 10^{-2}$	$0.77 \cdot 10^{-2}$	$0.49 \cdot 10^{-2}$
	$\boldsymbol{\psi_o}$ **(deg)**	0	0	0	0	0
CPC + IPC_I1ψ	$\overline{\mathbf{DEL}}$**(M) (MNm)**	14.32	14.67	16.33	17.22	13.45
	$\mathbf{k_t}$ **(deg/(MNms))**	$5.74 \cdot 10^{-2}$	$9.19 \cdot 10^{-2}$	$13.82 \cdot 10^{-2}$	$9.07 \cdot 10^{-2}$	$11.63 \cdot 10^{-2}$
	$\mathbf{k_y}$ **(deg/(MNms))**	$5.74 \cdot 10^{-2}$	$9.19 \cdot 10^{-2}$	$13.82 \cdot 10^{-2}$	$9.07 \cdot 10^{-2}$	$11.63 \cdot 10^{-2}$
	$\boldsymbol{\psi_o}$ **(deg)**	85.86	74.8	61.05	79.89	76.52
CPC + IPC_I2	$\overline{\mathbf{DEL}}$**(M) (MNm)**	16.8	16.25	18.23	20.07	15.96
	$\mathbf{k_t}$ **(deg/(MNms))**	$3.39 \cdot 10^{-2}$	$2.21 \cdot 10^{-2}$	$1.93 \cdot 10^{-2}$	$2.79 \cdot 10^{-2}$	$0.068 \cdot 10^{-2}$
	$\mathbf{k_y}$ **(deg/(MNms))**	$1.82 \cdot 10^{-2}$	$1.08 \cdot 10^{-2}$	$0.21 \cdot 10^{-2}$	$0.14 \cdot 10^{-2}$	$1.86 \cdot 10^{-2}$
	$\boldsymbol{\psi_o}$ **(deg)**	0	0	0	0	0
CPC + IPC_I2ψ	$\overline{\mathbf{DEL}}$**(M) (MNm)**	14.32	14.61	16.12	17.22	13.45
	$\mathbf{k_t}$ **(deg/(MNms))**	$5.73 \cdot 10^{-2}$	$19.4 \cdot 10^{-2}$	$11.65 \cdot 10^{-2}$	$8.93 \cdot 10^{-2}$	$12.28 \cdot 10^{-2}$
	$\mathbf{k_y}$ **(deg/(MNms))**	$5.76 \cdot 10^{-2}$	$12.9 \cdot 10^{-2}$	$20.14 \cdot 10^{-2}$	$9.55 \cdot 10^{-2}$	$11.01 \cdot 10^{-2}$
	$\boldsymbol{\psi_o}$ **(deg)**	88.75	75.33	62.27	77.50	76.85

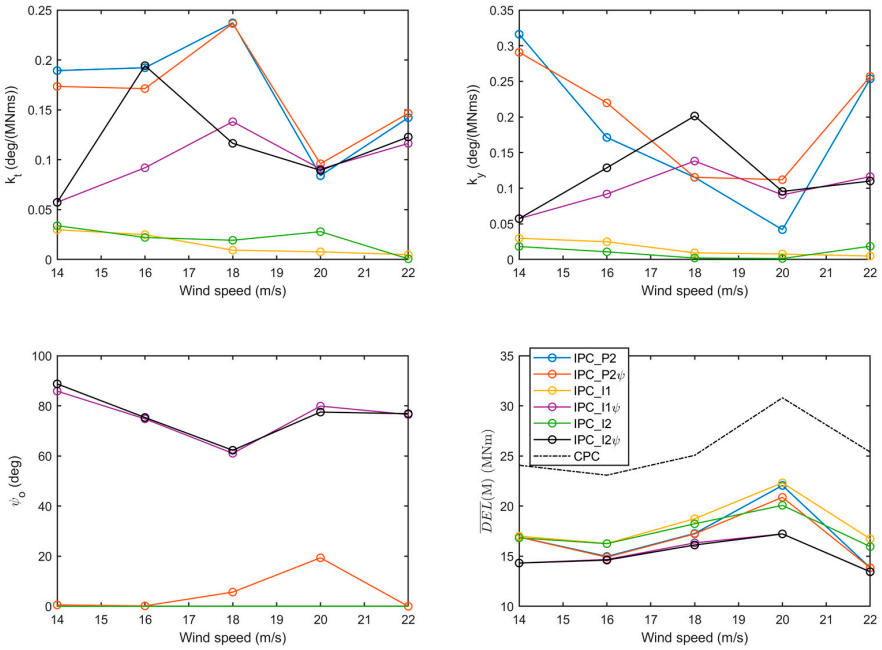

Figure 6. Graphical representation of the optimization results shown in Table 3: controller gains k_t and k_y, azimuth offset, and mean DEL value of the OoP blade moments with respect to the five mean wind speeds considered in the nominal region. The units of k_t and k_y gains are in deg/(MNm) for the IPC_P2 and IPC_P2ψ cases.

4.2. Simulation Results in the Rotating Reference Frame

The response of the previously designed IPC schemes is evaluated in this section. Three simulations were run with different wind profiles that included a stochastic turbulent component. The mean wind speed varied within the full load region. These different wind conditions were analyzed to study the performance of the proposed adaptive IPCs and their robustness. Wind profiles were created with the assistance of TurbSim in accordance with the IEC 61400-1 standard. The simulation time was 1200 s; however, the first 200 s were removed to discard transient effects in the data. In the first simulation (case 1), the average wind speed component ranged between 14 and 18 m/s. In case 2, the average wind speed varied between 16 and 20 m/s, and in case 3, between 18 and 22 m/s. The most significant variables in both the time and frequency domains were analyzed using the data obtained from each control strategy. Additionally, for each control strategy, various performance indicators related to blade moments, generated power, generator rotational speed, and pitch actuator effort were quantified. In the analysis, a reimplementation of the ROSCO CPC in Simulink without considering IPC was employed as the baseline control for comparison.

Figure 7 shows the simulated time responses of some proposed IPC schemes compared with the baseline CPC for simulation case 2. For clarity, only three IPC schemes are shown: the IPC with two different proportional controllers plus the azimuth offset (IPC_P2ψ), the IPC with two different integral controllers without the azimuth offset (IPC_I2), and the IPC with two identical integral controllers plus the azimuth offset (IPC_I1ψ). Also for clarity, only 250 s of the simulations are shown. Tables 4 and 5 present several performance indicators of the different control schemes for quantitative analysis; they were calculated for each case from the 1000 s simulation data.

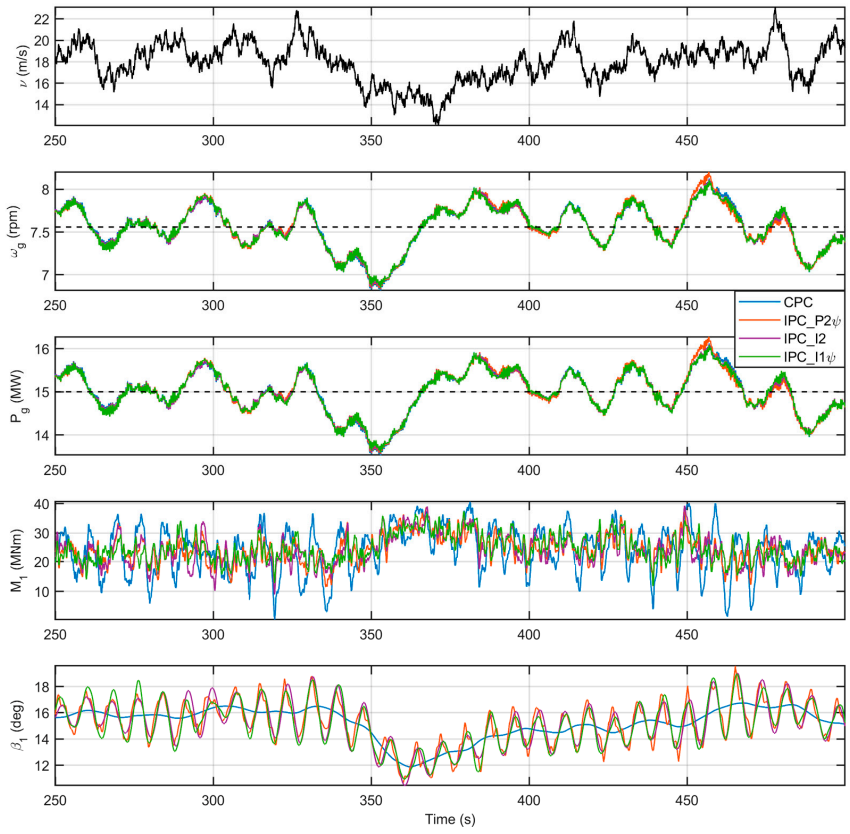

Figure 7. Time responses in the rotating reference frame of wind speed (ν), generator angular velocity (ω_g), generated power (P_g), OoP moment of blade 1, and pitch signal of blade 1 for simulation case 2 from 250 s to 500 s.

Table 4. Performance indicators of variables in the rotating reference frame for the control schemes were calculated from the simulation data for each simulation case. The table shows the average DEL value of the OoP blade moment ($\overline{\text{DEL}}$(M)), the average normalized actuator travel of the pitch ($\overline{\text{NAT}}$(β)), the STD of the generated power, and the STD of the generator angular velocity.

Control Scheme	$\overline{\text{DEL}}$(M) (MNm)			$\overline{\text{NAT}}$(β) (%)			STD(P_g) (MW)			STD(ω_g) (rpm)		
	Case 1	Case 2	Case 3	Case 1	Case 2	Case 3	Case 1	Case 2	Case 3	Case 1	Case 2	Case 3
CPC	23.67	25.62	29.68	4.91	4.38	4.07	0.46	0.60	0.80	0.23	0.30	0.40
CPC + IPC_P2	17.55	18.79	20.45	48.9	52.5	50.61	0.46	0.61	0.81	0.23	0.31	0.41
CPC + IPC_P2ψ	17.50	18.71	19.72	50	52.3	51.57	0.46	0.61	0.81	0.23	0.31	0.41
CPC + IPC_I1	18.80	21.94	21.68	41.6	44.6	46.45	0.46	0.61	0.80	0.23	0.31	0.40
CPC + IPC_I1ψ	16.60	17.25	17.51	38.8	43.4	49.45	0.46	0.60	0.81	0.23	0.30	0.41
CPC + IPC_I2	18.77	20.3	21.63	41.0	42.2	46.64	0.46	0.60	0.80	0.23	0.30	0.41
CPC + IPC_I2ψ	16.66	17.18	17.47	39.6	43.8	49.47	0.46	0.61	0.81	0.23	0.30	0.41

Table 5. The mean values and STD values of the non-rotating moments M_t and M_y were calculated from the simulation data for each simulation case.

Control Scheme	$\overline{M}_t$(MNm)			STD(M_t) (MNm)			$\overline{M}_y$(MNm)			STD(M_y) (MNm)		
	Case 1	Case 2	Case 3	Case 1	Case 2	Case 3	Case 1	Case 2	Case 3	Case 1	Case 2	Case 3
CPC	6.678	7.516	9.282	3.84	3.89	4.17	2.582	3.298	3.568	3.50	4.02	4.17
CPC + IPC_P2	−0.208	−0.252	0.118	2.86	3.15	3.62	−0.294	−0.067	−0.207	2.73	3.22	3.55
CPC + IPC_P2ψ	−0.209	−0.27	0.158	2.86	3.15	3.61	−0.219	0.588	1.202	2.70	3.19	3.42
CPC + IPC_I1	−0.015	−0.038	0.024	3.37	4.53	4.36	0.039	−0.072	0.100	3.46	4.61	3.97
CPC + IPC_I1ψ	−0.004	−0.008	−0.006	2.56	2.76	3.25	−0.011	−0.002	−0.013	2.24	2.45	2.89
CPC + IPC_I2	−0.06	−0.032	0.018	3.30	3.52	3.83	−0.015	0.247	0.188	3.91	4.84	4.43
CPC + IPC_I2ψ	−0.002	−0.004	−0.003	2.64	2.86	3.24	−0.008	−0.007	−0.011	2.33	2.59	2.87

Figure 7 shows the following variables in the rotating reference frame: wind speed, generator angular velocity, generated power, OoP moment of blade 1, and pitch signal of blade 1. The corresponding performance indicators are presented in Table 4, showing the average DEL value of the OoP blade moments, the average normalized actuator travel (NAT) of the pitch signals, the standard deviation (STD) of the generated power, and the STD of the generator rotational speed. The average NAT of the pitch signals is a measure of the average total traveled pitch angle and is defined as follows:

$$\overline{NAT}(\beta) = \frac{1}{3}\sum_{i=1}^{3}\left(\frac{1}{T}\int_0^T \left|\frac{\dot{\beta}_i(t)}{\dot{\beta}_{max}}\right| dt\right). \quad (10)$$

There were no significant differences, neither qualitatively nor quantitatively, between the control schemes in either the power generated or the generator speed, which indicates that the IPCs do not affect the response of the CPC loop. The STDs of P_g and ω_g of the different control schemes were practically the same in each case. The average P_g, not shown in Table 4, was also the same for the different schemes. The average generated power was 15.015 MW for case 1, 15.037 MW for case 2, and 15.021 for case 3.

In contrast, there were significant differences in the variables mainly related to the IPC loop. The baseline CPC showed the greatest oscillations of the OoP blade moment, whereas the IPCs managed to considerably mitigate the amplitude of these oscillations, as shown in Figure 7. Similar responses were obtained from the other simulation cases. Quantitatively, the CPC had the highest $\overline{\text{DEL}}$(M) value for all cases, as shown in Table 4. All the proposed IPC schemes reduced these DEL values. In simulation cases 1 and 2, the IPC schemes with integral controllers plus the azimuth offset achieved a greater reduction in the DEL value of 30% compared to the CPC, whereas those same IPC schemes without the azimuth only achieved a reduction of approximately 15–20%. With proportional controllers in the IPC, the reduction in the DEL was 25%, and the inclusion of the azimuth offset did not improve this value. In simulation case 3, the two IPC schemes with integral controllers

and azimuth offset achieved a DEL reduction of 40%. This reduction was only 27% for IPC schemes with integral controllers without azimuth offset and 32% for IPC schemes with proportional controllers.

The IPC schemes achieve this reduction in the DEL at the cost of greater control effort on the pitch actuators compared with the CPC. Figure 7 shows this greater activity in the pitch signal of blade 1. This is also indicated by the average normalized actuator travel indices ($\overline{NAT}(\beta)$) shown in Table 4, which increased from values of around 5% to between 40% and 50%. If we compare the IPC schemes with each other, the schemes with integral controllers plus the azimuth offset are the ones that, in addition to the greatest reduction in DEL, had the lowest NAT values, which were between 2% and 4% lower than those of the IPC schemes without the azimuth offset. The IPC schemes with proportional controllers showed the highest NAT values, which were as much as 10% higher than those of the other IPC schemes.

4.3. Simulation Results in the Non-Rotating Reference Frame

This section analyzes the internal variables of the IPC in the non-rotating reference system for the simulations performed in the previous section. Figure 8 shows the temporal response of these variables for simulation case 2. These variables are the tilt and yaw moments (M_t and M_y) obtained by the MBC transform, the tilt and yaw pitch signals (β_t and β_y), and the evolution of the adaptive gains k_t and k_y of the controllers and the adaptive azimuth offset ψ_o. As in Figure 7, for clarity, only three IPC schemes and only 250 s of simulation are shown. Table 5 shows the mean values and STDs of the moments M_t and M_y for the three simulation cases.

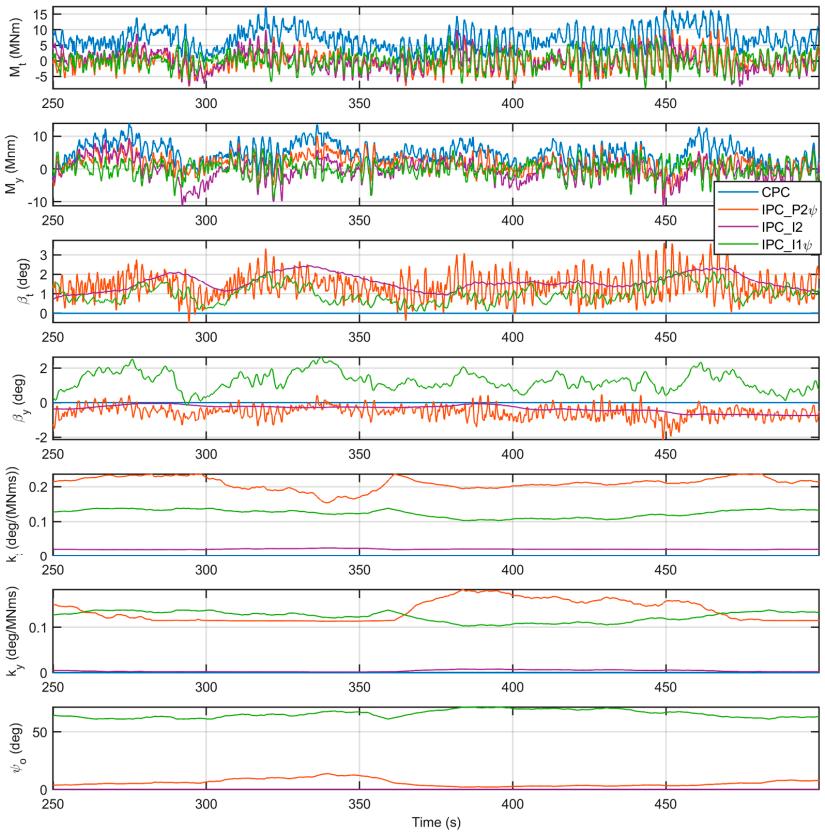

Figure 8. Time responses of the IPC variables in the non-rotating reference frame: tilt moment (M_t), yaw moment (M_y), tilt pitch signal (β_t), yaw pitch signal (β_y), controller adaptive gains (k_t and k_y), and adaptive azimuth offset (ψ_o) for simulation case 2 from 250 s to 500 s. The units of k_t and k_y gains are in deg/(MNm) for IPC_P2ψ.

The CPC without IPC showed an average component of the moments M_t and M_y far away from zero, which negatively impacted the DEL value of the OoP blade moments. IPC schemes significantly reduced the mean of these moments by approximately 99%, especially the IPC with integral controllers. The IPC schemes that reduced these mean values the most were those with integral controllers plus the azimuth offset (IPC_I1ψ and IPC_I2ψ), as shown in Table 5. The IPCs with proportional controllers required much higher activity of the pitch signals in the non-rotating frame (β_t and β_y) to reduce these moments and still showed higher mean values of these moments. The IPC adaptive gains k_t and k_y agree with the calculations in the previous section. The IPC schemes with proportional controllers showed higher gains than the IPC schemes with integral controllers, and their azimuth offset values were much lower than those of the IPC schemes with integral action. Among the IPC schemes with integral controllers, those with the azimuth offset had higher controller gains.

4.4. Frequency Response

Next, three of the proposed IPC schemes and CPC were compared in the frequency domain. For blade 1, Figure 9 shows the Fourier spectrum of the OoP blade bending moment M_1 on the left and the pitch signal β_1 on the right. The IPC schemes significantly decreased the large peak of the 1P component of the OoP moment M_1 around the frequency of 0.126 Hz when compared with the CPC scheme. The IPC_I1ψ virtually removed this peak. Regarding pitch signals, CPC without the IPC did not display 1P peaks; however, all IPC schemes showed a significant peak associated with the 1P pitch component, which was primarily responsible for the greater pitch effort.

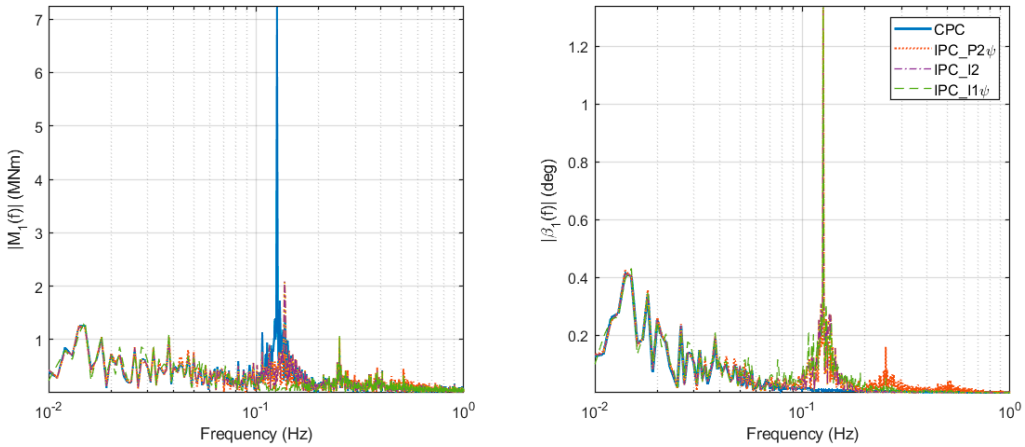

Figure 9. Frequency domain response of the out-of-plane blade moment and pitch signal for blade 1 using Fourier spectra.

Based on the analysis performed in this section, when the IPC schemes are optimally tuned to decrease the DEL of OoP blade moments, we can state the following: (1) The IPC schemes with integral controllers without the azimuth offset had roughly the same performance as the IPC schemes with proportional controllers (with or without the azimuth offset), (2) using identical or different gains in the decentralized controllers of IPC did not have a significant impact, (3) including the azimuth offset in the IPC schemes with integral actions helped to reduce the DEL value by a further 10%, and (4) including the azimuth offset in the IPC schemes with proportional controllers did not show significant improvements.

5. Conclusions

In this study, we analyze and compare the real improvements that can be achieved with different types of adaptive controllers with the azimuth offset and different controller gains in different IPC schemes tested on a 15 MW wind turbine model, which is simulated with OpenFAST v3.5 software. The problem of controller parameter tuning is addressed as

an optimization where the fatigue load on the blade is minimized according to the DEL and solved by genetic algorithms. The proposed IPC schemes are implemented as an adaptive block where the gains and azimuth offset have scheduled values according to the mean value of the filtered moments of the blades. In addition, the IPC schemes are combined with a pre-defined CPC. Several simulations are performed to compare the proposed IPC schemes. Specifically, we analyze the impact of three aspects: using proportional or integral controllers, using two identical or two different gains in the decentralized controllers of the IPC, and including or not including the azimuth offset in the reverse MBC transform. There is previous research on the impact of including the offset or not in the control; however, we have not found any works in the literature that simultaneously analyze the impact of the three factors considered here on control performance.

The simulation findings show that the proposed methodology is robust and adaptable to wind conditions and that it may be utilized to improve the structural integrity of blade wind turbines without sacrificing power generation efficiency. The IPC schemes proposed in this work significantly decrease the out-of-plane (OoP) blade moments when compared to not using IPC but at the cost of greater pitch actuator effort. A comparison of the proposed IPC schemes demonstrates that:

- The optimal IPC solution with proportional controllers (with or without the azimuth offset) produces a similar reduction in DEL values as the optimal solution of IPC with integral controllers without the azimuth offset; however, the proportional controllers produce higher pitch signal activity.
- The IPC schemes with integral controllers and the azimuth offset outperform the other schemes because they achieve the lowest DEL values of the OoP blade moments with minor pitch activity.
- Using different gains in the controllers of the IPC does not provide significant improvements; however, it requires an additional tuning parameter in the optimization procedure and, consequently, a higher computational cost.

Therefore, we can conclude that the most advantageous IPC scheme is the IPC_I1ψ case—that is, the IPC with two optimal identical integral controllers plus an optimal azimuth offset—because it surpasses the response of the other optimized IPC schemes and requires only two parameters to be tuned. This IPC scheme can achieve an additional reduction of approximately 10% in the DEL value of the OoP blade moments with the lowest pitch actuator effort in comparison with the other IPC schemes.

Future research is required to deal with the trade-off between the two main conflicting objectives in IPC: blade load reduction and pitch actuator effort. Future work will also address the analysis of more advanced controllers in the IPC scheme, such as multi-loop PI or PID controllers, H_∞ control, and decoupling control.

Author Contributions: Conceptualization, M.L., S.P.M. and J.-W.v.W.; methodology, M.L. and S.P.M.; software, M.L.; validation, S.P.M., J.-W.v.W., F.V. and J.G.; formal analysis, M.L.; investigation, M.L. and J.G.; resources, F.V. and J.G.; data curation, J.G.; writing—original draft preparation, J.G.; writing—review and editing, J.G., S.P.M., J.-W.v.W. and M.L.; visualization, J.G.; supervision, J.-W.v.W. and F.V.; project administration, J.G.; funding acquisition, J.G. and F.V. All authors have read and agreed to the published version of the manuscript.

Funding: This research was funded by the Spanish Ministry of Science and Innovation (MCIN/AEI/10.13039/501100011033), grant number PID2020-117063RB-I00. The APC was funded by PID2020-117063RB-I00.

Institutional Review Board Statement: Not applicable.

Informed Consent Statement: Not applicable.

Data Availability Statement: The data presented in this study are openly available in Mendeley Data, V1, at https://data.mendeley.com/datasets/7s3vxhzm8y/1 (accessed on 23 December 2023).

Acknowledgments: Manuel Lara expresses appreciation for the FPU fellowship (FPU17/02747) from the Spanish Ministry of Education, Culture, and Sports.

Conflicts of Interest: The authors declare no conflicts of interest. The funders had no role in the design of the study; in the collection, analyses, or interpretation of data; in the writing of the manuscript; or in the decision to publish the results.

Abbreviations

The following abbreviations, acronyms, and symbols are used in this manuscript:

CPC	Collective pitch control
DEL	Damage equivalent load
GA	Genetic algorithm
I	Integral
IEC	International Electrotechnical Commission
IPC	Individual pitch control
IPC_P2	IPC with two different proportional controllers and no azimuth offset
IPC_P2ψ	IPC with two different proportional controllers and the azimuth offset
IPC_I1	IPC with two identical integral controllers and no azimuth offset
IPC_I1ψ	IPC with two identical integral controllers and the azimuth offset
IPC_I2	IPC with two different integral controllers and no azimuth offset
IPC_I2ψ	IPC with two different integral controllers and the azimuth offset
MBC	Multi-blade coordinate
NAT	Normalized actuator travel
NREL	National Renewable Energy Laboratory
OoP	Out-of-plane
P	Proportional
PI	Proportional–integral
ROSCO	Reference open-source controller
RWT	Reference wind turbine
STD	Standard deviation
VS-VP	Variable speed, variable pitch
C_t	Tilt moment controller
C_y	Yaw moment controller
J	Cost function
k_t	Gain of tilt moment controller
k_y	Gain of yaw moment controller
M_i, M_{yi}	Out-of-plane moment of blade i
M_{xi}	In-plane moment of blade i
M_t	Tilt moment (in the nonrotating frame)
M_y	Yaw moment (in the nonrotating frame)
$P_{g,rated}$	Rated generated power
P_g	Generated power
S	Solution space
T_g	Generator torque
$T_{g,rated}$	Rated generator torque
T(ψ)	MBC transform matrix
T^{-1}	Reverse MBC transform
k_t	Gain of tilt moment controller
k_y	Gain of yaw moment controller
s	Laplacian variable
t	Time
β_i	Pitch command value of blade i
β_{CPC}	Pitch angle provided by the CPC
β_{IPCi}	IPC component for pitch signal of blade i
β_t	Tilt pitch angle (in the nonrotating frame)
β_y	Yaw pitch angle (in the nonrotating frame)

ρ	Decision variable vector
ψ_i	Azimuth angle of blade i
ψ_o	Azimuth offset
ψ	Vector with the three azimuth angles
ν	Mean wind speed
ω_g	Rotational generator speed
$\omega_{g,rated}$	Rated rotational generator speed

References

1. Njiri, J.G.; Söffker, D. State-of-the-Art in Wind Turbine Control: Trends and Challenges. *Renew. Sustain. Energy Rev.* **2016**, *60*, 377–393. [CrossRef]
2. Lee, J.; Zhao, F. *GWEC Global Wind Report*; Global Wind Energy Council: Brussels, Belgium, 2022; p. 75.
3. European Commission. *The Commission Calls for a Climate Neutral Europe by 2050*; European Commission: Brussels, Belgium, 2018.
4. Bossanyi, E.A. Individual Blade Pitch Control for Load Reduction. *Wind Energy* **2003**, *6*, 119–128. [CrossRef]
5. Jeong, J.; Park, K.; Jun, S.; Song, K.; Lee, D.-H. Design Optimization of a Wind Turbine Blade to Reduce the Fluctuating Unsteady Aerodynamic Load in Turbulent Wind. *J. Mech. Sci. Technol.* **2012**, *26*, 827–838. [CrossRef]
6. Cheon, J.; Kim, J.; Lee, J.; Lee, K.; Choi, Y. Development of Hardware-in-the-Loop-Simulation Testbed for Pitch Control System Performance Test. *Energies* **2019**, *12*, 2031. [CrossRef]
7. Mulders, S.P.; Pamososuryo, A.K.; Disario, G.E.; van Wingerden, J.-W. Analysis and Optimal Individual Pitch Control Decoupling by Inclusion of an Azimuth Offset in the Multiblade Coordinate Transformation. *Wind Energy* **2019**, *22*, 341–359. [CrossRef]
8. Lu, Q.; Bowyer, R.; Jones, B.L. Analysis and Design of Coleman Transform-Based Individual Pitch Controllers for Wind-Turbine Load Reduction. *Wind Energy* **2015**, *18*, 1451–1468. [CrossRef]
9. Mulders, S.P.; van Wingerden, J.-W. On the Importance of the Azimuth Offset in a Combined 1P and 2P SISO IPC Implementation for Wind Turbine Fatigue Load Reductions. In Proceedings of the IEEE 2019 American Control Conference (ACC), Philadelphia, PA, USA, 10–12 July 2019; pp. 3506–3511.
10. Spencer, M.D.; Stol, K.A.; Unsworth, C.P.; Cater, J.E.; Norris, S.E. Model Predictive Control of a Wind Turbine Using Short-Term Wind Field Predictions. *Wind Energy* **2013**, *16*, 417–434. [CrossRef]
11. Sierra-García, J.E.; Santos, M. Performance Analysis of a Wind Turbine Pitch Neurocontroller with Unsupervised Learning. *Complexity* **2020**, *2020*, 4681767. [CrossRef]
12. Sierra-Garcia, J.E.; Santos, M. Improving Wind Turbine Pitch Control by Effective Wind Neuro-Estimators. *IEEE Access* **2021**, *9*, 10413–10425. [CrossRef]
13. Mulders, S.; Pamososuryo, A.; van Wingerden, J. Efficient Tuning of Individual Pitch Control: A Bayesian Optimization Machine Learning Approach. *J. Phys. Conf. Ser.* **2020**, *1618*, 022039. [CrossRef]
14. Lara, M.; Garrido, J.; van Wingerden, J.-W.; Mulders, S.P.; Vázquez, F. Optimization with Genetic Algorithms of Individual Pitch Control Design with and without Azimuth Offset for Wind Turbines in the Full Load Region. *IFAC-PapersOnLine* **2023**, *56*, 342–347. [CrossRef]
15. Ragan, P.; Manuel, L. Comparing Estimates of Wind Turbine Fatigue Loads Using Time-Domain and Spectral Methods. *Wind Eng.* **2007**, *31*, 83–99. [CrossRef]
16. Gaertner, E.; Rinker, J.; Sethuraman, L.; Zahle, F.; Anderson, B.; Barter, G.; Abbas, N.; Meng, F.; Bortolotti, P.; Skrzypinski, W.; et al. *Definition of the IEA Wind 15-Megawatt Offshore Reference Wind Turbine Technical Report*; National Renewable Energy Laboratory: Golden, CO, USA, 2020.
17. NREL OpenFAST v3.4.1 Documentation. Available online: https://openfast.readthedocs.io/en/main/ (accessed on 24 April 2023).
18. Niranjan, R.; Ramisetti, S.B. Insights from Detailed Numerical Investigation of 15 MW Offshore Semi-Submersible Wind Turbine Using Aero-Hydro-Servo-Elastic Code. *Ocean Eng.* **2022**, *251*, 111024. [CrossRef]
19. Papi, F.; Bianchini, A. Technical Challenges in Floating Offshore Wind Turbine Upscaling: A Critical Analysis Based on the NREL 5 MW and IEA 15 MW Reference Turbines. *Renew. Sustain. Energy Rev.* **2022**, *162*, 112489. [CrossRef]
20. Jonkman, J.; Butterfield, S.; Musial, W.; Scott, G. *Definition of a 5-MW Reference Wind Turbine for Offshore System Development*; National Renewable Energy Lab., (NREL): Golden, CO, USA, 2009.
21. KC, A.; Whale, J.; Evans, S.P.; Clausen, P.D. An Investigation of the Impact of Wind Speed and Turbulence on Small Wind Turbine Operation and Fatigue Loads. *Renew. Energy* **2020**, *146*, 87–98. [CrossRef]
22. Jonkman, B. *TurbSim User's Guide: Version 1.50*; National Renewable Energy Lab., (NREL): Golden, CO, USA, 2009.
23. *IEC 61400-1*; Wind Turbines—Part 1: Design Requirements. IEC: Geneva, Switzerland, 2005.
24. Novaes Menezes, E.J.; Araújo, A.M.; Bouchonneau da Silva, N.S. A Review on Wind Turbine Control and Its Associated Methods. *J. Clean. Prod.* **2018**, *174*, 945–953. [CrossRef]
25. Abbas, N.J.; Zalkind, D.S.; Pao, L.; Wright, A. A Reference Open-Source Controller for Fixed and Floating Offshore Wind Turbines. *Wind Energy Sci.* **2022**, *7*, 53–73. [CrossRef]
26. Serrano, C.; Sierra-Garcia, J.-E.; Santos, M. Hybrid Optimized Fuzzy Pitch Controller of a Floating Wind Turbine with Fatigue Analysis. *J. Mar. Sci. Eng.* **2022**, *10*, 1769. [CrossRef]

27. NREL MLife | Wind Research | NREL. Available online: https://www.nrel.gov/wind/nwtc/mlife.html (accessed on 25 April 2023).
28. Deb, K. An Efficient Constraint Handling Method for Genetic Algorithms. *Comput. Methods Appl. Mech. Eng.* **2000**, *186*, 311–338. [CrossRef]
29. Andrade Aimara, G.A.; Esteban San Román, S.; Santos, M. Control Tuning by Genetic Algorithm of a Low Scale Model Wind Turbine. In Proceedings of the International Workshop on Soft Computing Models in Industrial and Environmental Applications, Salamanca, Spain, 5–7 September 2023; pp. 515–524.